Electrochimica Acta 174 (2015) 332–339

Contents lists available at ScienceDirect

Electrochimica Acta

journal homepage: www.elsevier.com/locate/electacta

Reduced graphene oxide-Sb_2O_5 hybrid nanomaterial for the design of a laccase-based amperometric biosensor for estriol

Fernando H. Cincotto[a,b], Thiago C. Canevari[c,*], Sergio A.S. Machado[b], Alfredo Sánchez[a], Maria Asunción Ruiz Barrio[a], Reynaldo Villalonga[a,*], José M. Pingarrón[a,*]

[a] Department of Analytical Chemistry, Faculty of Chemistry, Complutense University of Madrid, 28040 Madrid, Spain
[b] Institute of Chemistry, State University of São Paulo, PO Box 780, 13560-970 São Carlos, SP, Brazil
[c] Engineering School, Mackenzie Presbiterian University, 01302-907 São Paulo, SP, Brazil

ARTICLE INFO

Article history:
Received 26 April 2015
Received in revised form 2 June 2015
Accepted 2 June 2015
Available online 5 June 2015

Keywords:
Biosensor
estriol
graphene oxide
Sb_2O_5
hybrid material

ABSTRACT

A novel reduced graphene oxide/Sb_2O_5 hybrid nanomaterial was prepared by a one-pot reaction process. The nanomaterial was characterized by different spectroscopic, microscopic and electrochemical techniques, demonstrating that the graphene sheets were doped with a Sb_2O_5 thin film. A glassy carbon electrode coated with the hybrid material was further employed as support for the covalent immobilization of laccase to develop an electrochemical biosensor for estriol. The enzyme biosensor showed high sensitivity (275 mA/M) and fast analytical response (4 s) for the hormone, with a limit of detection of 11 nM in the range of 25 nM to 1.03 μM. The biosensor showed high selectivity for the analytical detection of estriol.

1. Introduction

The design of novel, highly sensitive, selective and stable electrochemical biosensors devices able to be used for the fast, accurate, reproducible, *in situ* and low cost analysis of chemical compounds with biomedical, forensic and environmental importance is a challenge in electroanalytical chemistry [1–3]. During last years, progresses in nanomaterials chemistry have empowered biosensor technology by providing a great variety of advanced nanomaterials for their use as transduction elements in electrochemical biosensors [4–7]. These nanosized materials have unique size-dependent properties that can be rationally manipulated to assemble original 3D arquitectures at electrode surfaces to ensure high yield of immobilized bioreceptor, easy electrocatalytic transformation of analytes and fast electron transfer processes at the sensing interface.

In this context, graphene and graphene oxide (GO) ranks among the nanomaterials more widely employed for the assembly of electrochemical biosensors due to their remarkable thermal, mechanical and electronic properties [8–10]. These carbon nanomaterials showing a planar two-dimensional morphology can be prepared at relative low cost and easily functionalized with a variety of chemical groups. Graphene and its oxidized derivative can be also combined with other materials and compounds, such as polymers, ceramics, metal and metal oxides nanostructures, etc., to yield novel composite or hybrid adducts with improved or new chemical and physical properties [11–13]. In this regard, the synergistic effect between graphene and metal oxide nanostructures in hybrid nanomaterials have opened new possibilities to design electrochemical biosensors with desired properties and behaviors [14].

Here we describe the preparation of a hybrid nanomaterial of reduced GO (rGO) and Sb_2O_5 and its use as transducer element for the construction of an electrochemical enzyme biosensor. Sb_2O_5 is a metal oxide widely employed in the synthesis of hybrid materials for electroanalytical purposes [15–17] due to its excellent acidic properties and surface defects which favor the incorporation of other species on its surface and the electrocatalytic transformation of relevant compounds. The selected target analyte to evaluate the suitability of the hybrid nanomaterial-based biosensor was estriol ((16α,17β)-estra-1,3,5(10)-triene-3,16,17-triol), a phenolic estrogen hormone widely used in the treatment of urogenital diseases in menopausal women. This drug, classified as endocrine disrupting compound [18,19], is commonly eliminated in the urine of patients and is not completely degraded during the treatment of sewage becoming a potential environmental risk [20]. The determination of estriol in human and environmental samples

* Corresponding authors. Tel.: +34 617597866.
E-mail addresses: tccanevari@gmail.com (T.C. Canevari), rvillalonga@quim.ucm.es (R. Villalonga), pingarro@quim.ucm.es (J.M. Pingarrón).

http://dx.doi.org/10.1016/j.electacta.2015.06.013
0013-4686/

has been mainly performed by gas and liquid chromatography [19,21–23] and spectrophotometric techniques [24–26], but these analytical procedures require exhaustive pre-treatment of samples prior to analysis. Several authors have proposed electroanalytical techniques as reliable alternatives for estriol detection [18,20,27], and succesful results have been achieved by using proper combination of new advanced materials and highly selective bioreceptor on the transducer interfase. In this case, laccase (EC 1.10.3.2) was employed as catalytic bioreceptor in this biosensor design due to its capacity to transform phenolic compounds, such as estriol, through oxidation reactions.

2. Experimental

2.1. Reagents

$SbCl_3$ was acquired from Merck. Graphite powder, laccase from *Trameters versicolor* (Lac, 10 U/mg) and the other chemicals were purchased from Sigma-Aldrich.

2.2. Apparatus, electrodes and solutions

The X-rays photoelectron spectra (XPS) were obtained with a VSW HA 100 hemispherical electron analyzer (VSW Scientific Instrument Ltda., UK). The XPS spectra were deconvoluted using the Gaussian-Lorentzian peak fitting using the software OriginPro 8.0 (OriginLab Co., USA). The nanohybrid morphology was investigated by atomic force microscopy (AFM) with a SPM Nanoscope IIIa multimode microscope (Veeco Instruments Inc., USA). High resolution field emission scanning electron microscopy (FE-SEM) was performed with a JEOL JSM-6335F microscope (JEOL Ltd., Japan). Transmission electron microscopy (TEM) and high resolution transmission electron microscopy (HRTEM) measurements were performed with JEOL JEM-2100 FX and JEOL JEM-3000 F microscopes, respectively (Jeol Ltd., Japan).

Amperometric measurements were performed with a dual-channel ultrasensitive Inbea potentiostat (Inbea Biosensores S.L., Spain). Cyclic voltammetry and electrochemical impedance spectroscopy experiments were performed using a FRA2 μAutolab Type III potentiostat/galvanostat (Metrohm Autolab B.V., The Netherlands). A conventional three-electrode system was employed in all electrochemical studies. The working electrode was a glassy carbon electrode (GCE, 3.0 mm diameter) modified with the graphene derivative and the immobilized enzyme. An Ag/AgCl/KCl (3 M) and a Pt wire were used as reference and counter electrodes, respectively. The measurements with the biosensor were carried out at 25 °C in 0.1 M sodium phosphate buffer, pH 7.0 (working volume 10 ml). Stock solutions of 1.0 mM estriol in ethanol, were freshly prepared.

2.3. Preparation of the rGO/Sb_2O_5 hybrid nanomaterial

GO was first prepared by modification of Hummers' method [28]. In brief, 10 g graphite and 10 g $NaNO_3$ were mixed in 450 mL of H_2SO_4 (98%) in a 2500 mL round-bottom flask immersed in an ice bath. The mixture was stirred for 30 min and then 60 g KMnO4 were added under vigorous stirring. The reaction mixture was held under refrigeration at 4 °C for 24 h. The temperature was further raised to 35 °C and the mixture was stirred for 1 h. Subsequently, H_2O_2 (30% v/v, 450 mL) was added under vigorous stirring, and the reaction temperature was rapidly increased to 98 °C. Water (450 mL) and H_2O_2 (30% v/v, 300 mL) were sequentially added under stirring, and the reaction mixture was refrigerated at 4 °C and stirred for other 24 h. The solution containing GO was centrifuged for 30 min at 8000 rpm and washed several times with 5% HCl (v/v) and distilled water until the pH of the filtrate was neutral. GO was finally lyophilized and kept under dry conditions until use.

To prepare the rGO/Sb_2O_5 hybrid nanomaterial, 80 mg GO, 10 mg $SbCl_3$ and 8 mg sodium dodecyl sulfate were mixed in 40 mL CCl_4 under Ar atmosphere. The mixture was stirred for 20 min and then 2 mL of 1.2×10^{-2} mol L^{-1} $NaBH_4$ were added. The mixture was refluxed at 70 °C for 2 h, then filtered and washed three times with CCl_4. The resulting nanomaterial was finally dried at 50 °C for 48 h.

2.4. Preparation of the enzyme electrode

A bare GCE was first polished to mirror-like surface with alumina powder (0.3 μm), rinsed thoroughly with double distilled water, successively washed with double distilled water, anhydrous ethanol and acetone in an ultrasonic bath, and dried under N_2 before use. Coating of the polished GCE was accomplished by depositing 10 μL of a 1.0 mg/mL aqueous dispersion of rGO/Sb_2O_5 on the electrode surface and allowing drying. The enzyme was further immobilized on the modified electrode by dropping 10 μL of a 3.0 mg/mL laccase solution in 100 mM sodium phosphate buffer, pH 7.0, and mixed with 10 μL of 3% (v/v) glutaraldehyde. The electrode was kept at 4 °C for 1 h, then washed several times with cold 100 mM sodium phosphate buffer, pH 7.0, and finally stored in refrigerator until use (Lac/rGO/Sb_2O_5/GCE).

3. Results and discussion

The procedure employed to prepare the hybrid nanomaterial and further assembly of the enzyme electrode is displayed in Scheme 1. Firstly, rGO/Sb_2O_5 was prepared by controlled oxidation of $SbCl_3$ with the oxygen functional groups (epoxy and carbonyl moieties) at the GO nanosheets [29]. Simultaneously, the as-

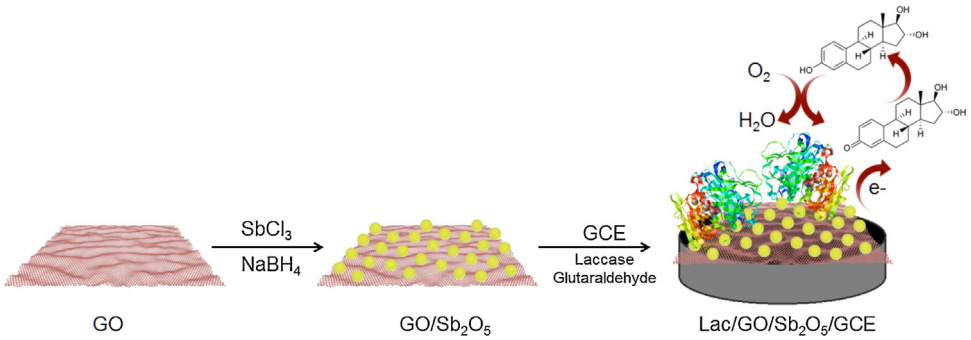

Scheme 1. Schematic display of the steps involved in the preparation of the rGO/Sb_2O_5 nanohybrid and the Lac/rGO/Sb_2O_5/GCE enzyme electrode.

growing nanonanomaterial was deposited on the rGO basal planes by interaction with the remaining oxygen functional groups (hydroxyl and carboxylic acid moieties) on the carbon nanomaterial. This chemical bonding is induced by the ability of reduced graphene oxide to act as catalytic agent for the chemical disproportionation of the antimony dopant layer which favors the charge transfer between the adsorbed antimony species and the rGO lattice [29,30]. The nanohybrid was then treated with $NaBH_4$ to ensure reduction of the partially reduced GO nanosheets. The resulting hybrid nanomaterial, upon deposition of GCE, was further employed as support for the glutaraldehyde-mediated covalent immobilization of laccase immobilization on the electrode surface to construct an amperometric enzyme biosensor for estriol.

The synthesized hybrid nanomaterial was characterized by different spectroscopic, microscopic and electrochemical techniques. XPS was used to obtain information about the chemical species and the oxidation states of antimony in the hybrid material. The complete spectrum of the rGO/Sb_2O_5 nanohybrid is shown in Figure 1S (Supporting information). Two intense peaks corresponding to the binding energy for oxygen (O1s) and carbon (C1S) are clearly observed in this spectrum. Peaks corresponding to silica, which was employed to make energy corrections, were also observed. Detailed study revealed the absence of peaks related to potential metal and non-metal contaminant species, suggesting high purity for the rGO/Sb_2O_5 nanohybrid. It should be highlighted that antimony binding energy is overlapped by oxygen binding energy, and accordingly, thorough analysis of this XPS spectrum should be performed.

To confirm the formation of antimony (V), and to simplify the analysis of the XPS spectra, all peaks were deconvoluted using the Gaussian–Lorentzian peak fitting. The results are shown in Fig. 1. In addition, a summary of the binding energy values for $Sb3d_{3/2}$, $Sb3d_{5/2}$, O1s, Sb4d and C1s is provided in Table 1S (Supporting information).

The peak of the binding energy for oxygen (O1s) overlaps the peak of the binding energy for the component $Sb3d_{5/2}$. Deconvolution of the spectrum reflected that the value around 534.2 eV was related to the $Sb3d_{5/2}$ component and the value around 532.5 eV could be ascribed to the O1s component. To confirm the formation of antimony (V), the analysis of the $Sb3d_{3/2}$ and Sb4d components were also performed. The values obtained for the binding energies of $Sb3d_{3/2}$ and Sb4d were 540.4 eV and 34.4 eV, respectively. These values were similar to those from pure Sb_2O_5 oxide, confirming the formation of antimony (V) oxide on the rGO sheets. The absence of binding energies for the $Sb3d_{3/2}$ and $Sb3d_{5/2}$ components around 539.7 eV and 530.7 eV also confirmed that antimony (III) oxide was not formed on the nanomaterial.

Deconvolution of the C1s component provided three values of binding energy (284.6 eV, 287 eV and 289.2 eV), indicating that GO had different functional groups. The value of the binding energy around 284.6 eV is related to the presence of hydroxyl groups attached to the carbon structure, the binding energy around 287 eV confirm the presence of C=O moieties and the binding energy around 289.2 eV can be ascribed to the carboxyl groups on the GO edges [25,31]. These data confirmed that the reduction with $NaBH_4$ was only able to reduce partially GO leaving remaining oxygen functional groups able to interact with Sb_2O_5.

The microstructural and morphological study of the hybrid material rGO/Sb_2O_5 was conducted by TEM, FE-SEM and AFM. Fig. 2 shows representative TEM images of GO before (A) and after modification Sb_2O_5 (B). The modified nanomaterial clearly showed dark zones that are dispersed on the rGO planar sheet, suggesting high coverage with Sb_2O_5. The presence of Sb in the rGO-based nanohybrid was confirmed by elemental analysis using Energy Dispersive Spectroscopy (EDS). As can be observed in Fig. 2C, the EDS spectrum showed the characteristics peaks of Sb with relative high intensity, suggesting high content of this metal in the hybrid nanomaterial. On the other hand, the nanohybrid showed a diffuse pattern when studied by selected area electron diffraction analysis (SAED) (inset in Fig. 2C). This fact suggests the Sb_2O_5 formed on the rGO sheets showed an amorphous structure. It is well know that the amorphous structure of Sb_2O_5 is characterized by the presence of Lewis & Bronsted acid sites on the material surface, thus conferring excellent properties to the rGO/Sb_2O_5 nanohybrid for the immobilization of biomolecules.

However, the presence of Sb_2O_5 nanoparticles was not evidenced by FE-SEM analysis (Fig. 3A), suggesting that the nanoparticles were too small to be observed by this technique. Accordingly, the nanohybrid was further studied by AFM, a more sensitive technique.

Fig. 4 shows the topological analysis of the rGO/Sb_2O_5 nanohybrid by AFM. The nanomaterial showed two different zones with well-defined topology. The non-modified zone showed the characteristic platelet-like morphology of rGO with 0.8-1.0 nm thick, in agreement with that reported for this material [32]. However, a noticeable increase in the thickness of the nanomaterial was observed on the modified zone suggesting the presence of the rGO/Sb_2O_5 nanohybrid with a thickness increase to about 1.5-2.2 nm in accordance with previous works [30]. In general, this hybrid nanomaterial showed high topological homogeneity, which was mainly characterized by the presence of single layer rGO nanosheets partially covered by the Sb_2O_5 nanostructure. However, the rGO nanosheets showed different size and degree of modification, as expected from the heterogeneous size distribution of the starting GO nanomaterial. In addition, some multilayered rGO/Sb_2O_5 hybrid nanostructures were observed by AFM analysis.

The rGO/Sb_2O_5 nanohybrid was employed as coating material for GCE to construct an enzyme electrochemical biosensor for estriol. Immobilization of laccase on the modified electrode

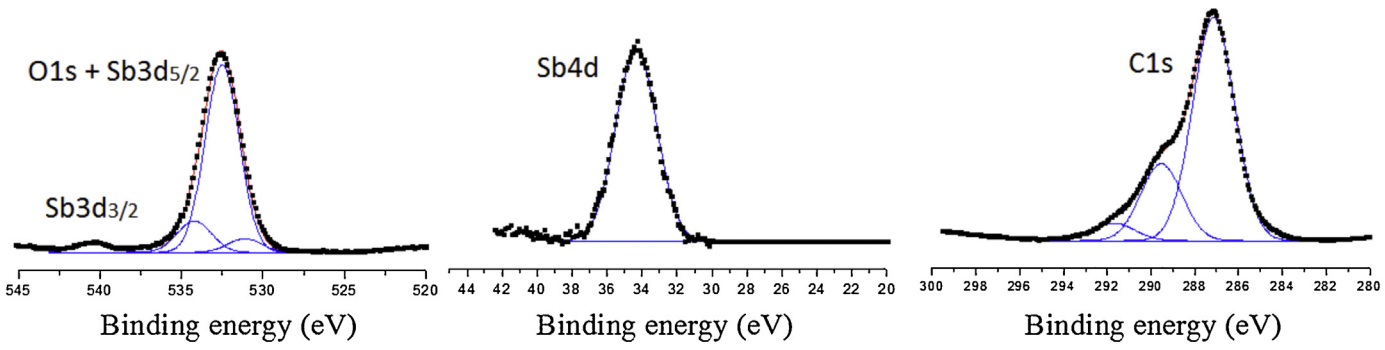

Fig. 1. XPS spectra of rGO/Sb_2O_5.

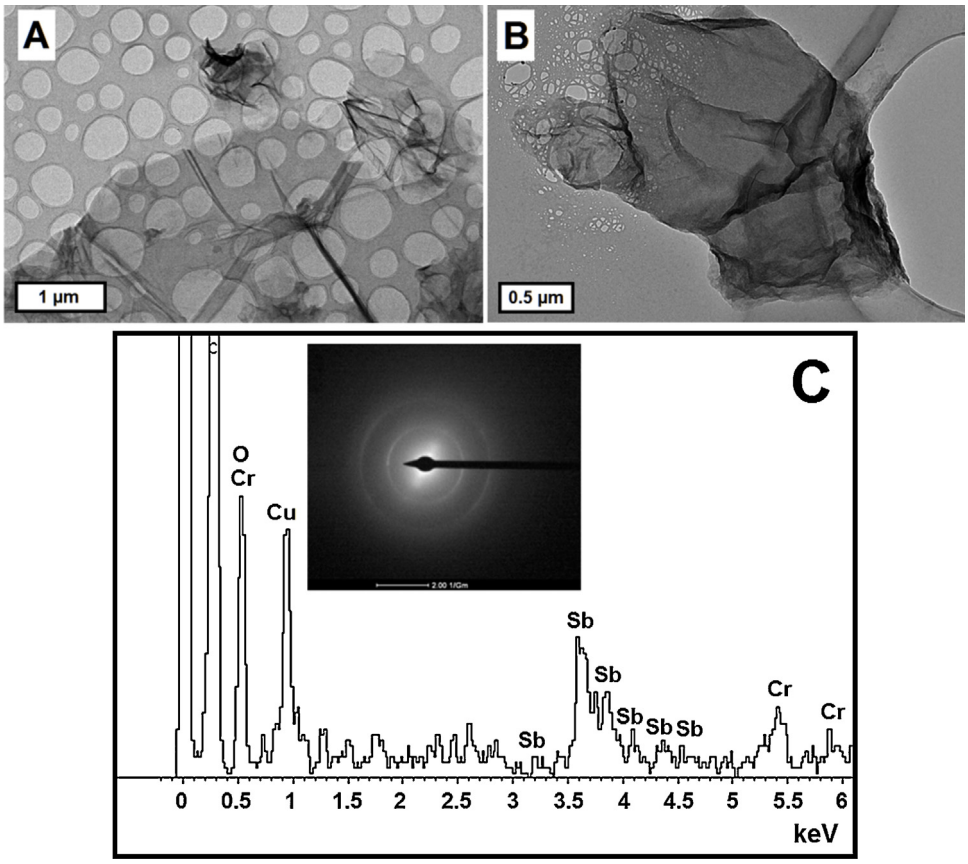

Fig. 2. TEM images of GO (A) and rGO/Sb_2O_5 (B). Elemental analysis (C) and selected area electron diffraction pattern (inset) of rGO/Sb_2O_5.

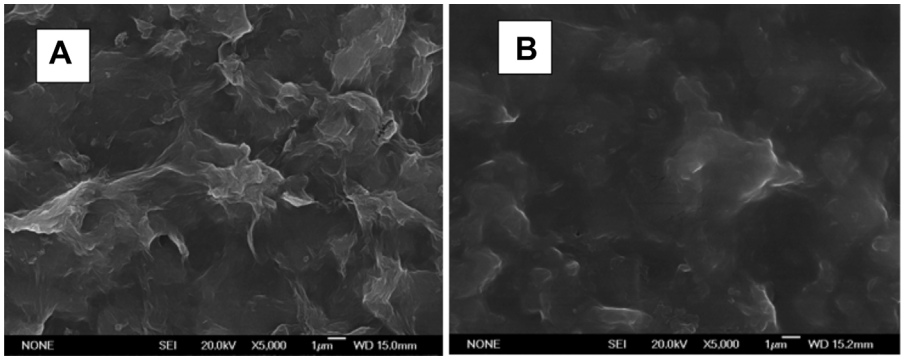

Fig. 3. FE-SEM image of rGO/Sb_2O_5 and Lac/rGO/Sb_2O_5.

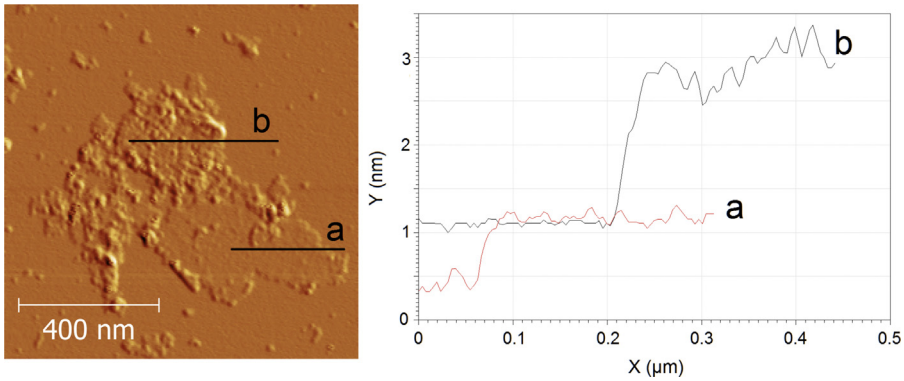

Fig. 4. AFM and section analysis for rGO/Sb_2O_5.

yielded a more amorphous surface, as revealed by FE-SEM analysis (Fig. 3B). This fact suggested high loading of enzyme protein molecules on the graphene-based hybrid nanomaterial. Optimization of experimental variables allowed us to conclude that higher electroanalytical responses of the enzyme electrode were achieved with 10 μL of 3 mg mL^{-1} laccase loading using 10 μL of 3% (v/v) glutaraldehyde (Figs. 2S-3S, respectively, Supporting information).

The assembly of the enzyme electrode was followed by electrochemical impedance spectroscopy (EIS), and the resulting Nyquist plots are shown in Fig. 5. Modification of the bare GCE with the graphene nanohybrid resulted in a non-significant increase in the electron transfer resistance (from 132 to 157 Ω), as it could be expected due to the high conductive properties of the graphene-based hybrid nanomaterial. The appearance of a second semicircle in the corresponding Nyquist plot suggested that the hybrid nanomaterial-coated electrode showed a non-homogeneous electrochemical interface. This EIS behavior could be justified by the non-homogeneous distribution of Sb_2O_5 on the rGO, as revealed by AFM analysis. Finally, the Lac/rGO/Sb_2O_5/GCE electrode showed a noticeable increase in the electron transfer resistance to 912 Ω, suggesting high coverage of the electrode surface by the laccase protein molecules, in agreement with SEM analysis.

The electrocatalytic activity of the Lac/rGO/Sb_2O_5/GCE enzyme electrode toward estriol was evaluated by cyclic voltammetry in 0.1 M PBS, pH 7 in the presence of 1.0 mM thionine as mediator which has been widely employed in the preparation of biosensors for phenolic compounds [33]. Bare GCE, rGO/Sb_2O_5 and Lac/GO coated GCEs were employed as control electrodes. As it can be observed in Fig. 6, the Lac/GO/GCE showed a little electrocatalytic effect for estriol, as revealed by the little increase in the cathodic current at potential values lower than -200 mV, suggesting low enzyme loading on this modified electrode. Similar cathodic currents were observed for the rGO/Sb_2O_5/GCE electrode, demonstrating the good electrocatalytic ability of the rGO-based hybrid nanomaterial. However, as expected, a remarkably better catalytic response for estriol was observed at the Lac/rGO/Sb_2O_5/GCE enzyme electrode, thus supporting the advantageous combination of the enzyme effect and the rGO-based nanohybrid transducer for the design of an electrochemical biosensor for this hormone.

Scheme 2 illustrates the electrocatalytic mechanism involved in the enzyme-mediated transformation of estriol at the electrode surface by using thionine as electrochemical mediator. Through this mechanism, estriol can be detected at relative low working

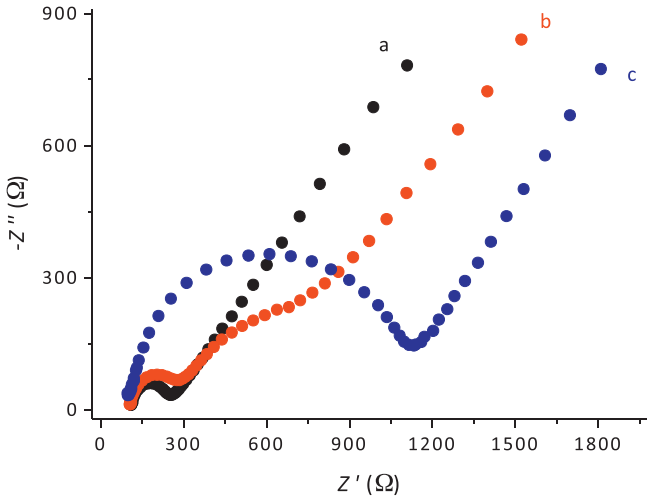

Fig. 5. Electrochemical impedance spectra obtained at a glassy carbon electrode before (a) and after coating with rGO/Sb_2O_5 (b) and further immobilization of laccase (c), in 0.1 M KCl solution containing 5 mM $K_3[Fe(CN)_6]/K_4[Fe(CN)_6]$ (1:1)

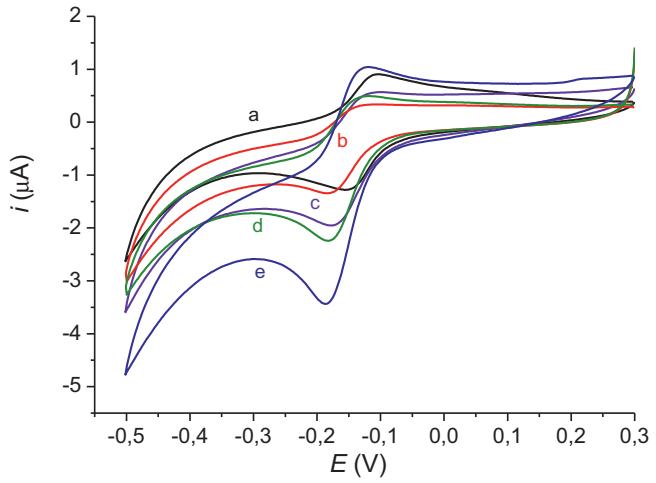

Fig. 6. Cyclic voltammograms recorded at the GCE (a), rGO/GCE (b), rGO/Sb_2O_5/GCE (c), Lac/GO/GCE (d) and Lac/rGO/Sb_2O_5/GCE (e) for 2.0 μM estriol in 0.1 M sodium phosphate buffer, pH 7.0, containing 1.0 mM thionine as mediator; v = 50 mV/s.

potential due to the capacity of thionine to mediate the transformation of this hormone at the nanostructured enzyme electrode surface.

Other working variables affecting the biosensor response were optimized. Regarding the concentration of mediator thionine in solution, the larger electrocatalytic response was observed for 1 mmol L^{-1} (Fig. 4S, Supporting information) and, accordingly, further experiments were performed under this condition. The influence of pH and the detection potential to be used on the amperometric response of the electrode to the target analyte were also evaluated. The results shown in Fig. 5S in supporting information indicated that higher electroanalytical responses were achieved by using a buffered solution of pH 7.0 and setting the working potential at -300 mV (Fig. 6S in Supporting information). Interestingly, a little increase in the electrocatalytic activity of laccase was observed at pH above 7.0 (Fig. 5S). This fact could be ascribed to changes in the ionization degree of the enzyme substrate (estradiol) and/or the electrochemical mediator (thionine) in alkaline media, allowing relative fast bioelectrochemical transformation on the laccase-modified electrode.

Under the optimized conditions, the enzyme electrode exhibited a fast amperometric response (4 s) upon continuous additions of the hormone (Fig. 7).

A linear calibration graph for estriol (r = 0.999) was obtained over the 25 nM to 1.03 μM range, with a slope value of 275 mA/M.

The limit of detection for this biosensor, 11 nM, was estimated according to the 3 s_b/m criterion, where s_b was estimated as the standard deviation of the mean current value measured for 10 blank solutions and m is the slope of the calibration plot.

Table 1 compares the analytical characteristics of the developed biosensors with other electrochemical reported in the recent literature.

According to Table 1, the Lac/rGO/Sb_2O_5/GCE biosensor for estriol hormone detection yields one of the lowest detection limits and a wide linear range by coupling the easy-to-prepare hybrid nanomaterial and the immobilization of laccase enzyme. This work represents the first proposal of an enzyme biosensor for electrochemical detection of estriol, suggesting the potential to improve the selectivity of the determination as leverage against others based on non-selective nanomaterials.

The selectivity of Lac/rGO/Sb_2O_5/GCE biosensor was evaluated by testing eight potential interfering species (hydroquinone, catechol, dopamine, progesterone, bysphenol A, 17β-estradiol, ethinylestradiol and ascorbic acid). In order to do that, the

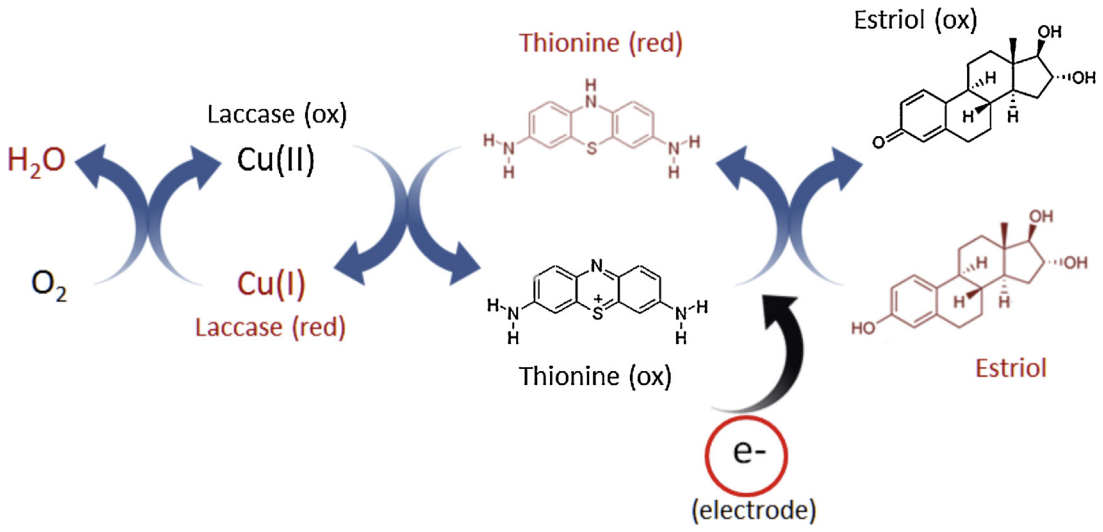

Scheme 2. Schematic display of the electrocatalytic mechanism for the enzyme biosensor.

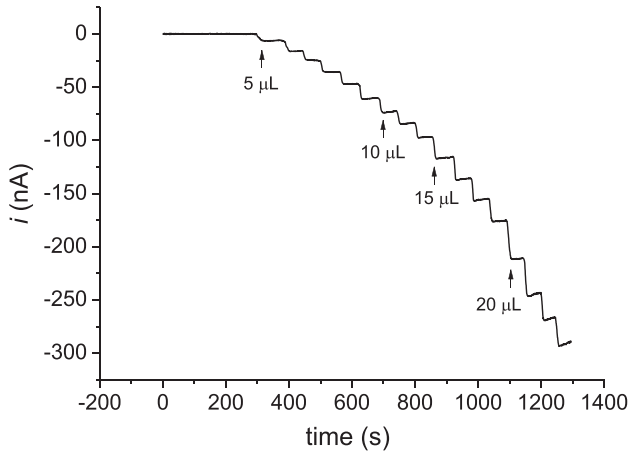

Fig. 7. Typical current–time responses for successive addition of 5.0×10^{-5} mol L^{-1} estriol in presence of 1.0 mmol L^{-1} thionine in 0.1 mol L^{-1} PBS (pH 7) at the Lac/rGO/Sb_2O_5/GCE. Estriol concentration range between 0.025 and 1.025 μmol L^{-1}.

amperometric response obtained with the biosensor for 1.0 μmol L^{-1} estriol was compared with those measured under the same conditions for 10 and 100 times this concentration of these potential interfering compounds. Table 2 summarizes the obtained results expressed as percentage of the signal recorded for the target analyte. As it can be deduced, a high selectivity of the Lac/rGO/Sb_2O_5/GCE biosensor for estriol was found. In fact, all the potential interfering compounds did not produce a noticeable amperometric response at a concentration level 10 times than that used for estriol. Only 17β-estradiol and ethinylestradiol at much larger concentration (100 times) produced responses of the same order than that for estriol which could be expected due to the similar structures of these compounds belonging to the same family of disrupting compounds.

The repeatability of the amperometric responses obtained with the biosensor was estimated by measuring ten successive additions of 1.0 μM estriol. The resulting RSD = 2.84% indicates good repeatability for this biosensor. Moreover, the reproducibility of the whole biosensor assembling process was tested by constructing five different electrodes using the same protocol. The RSD = 4.37% obtained by measuring the steady-state current for 1.0 μM estriol demonstrated high reliability for the fabrication procedure.

The long-term storage stability of the biosensor was also evaluated by measuring the response to 1.0 μM estriol during 2 months of storage at 4 °C under dry conditions. The biosensor retained about 84% of its original response after 1 month of storage and the electrocatalytic ability gradually decreased to about 52% after 2 months of storage. This storage stability can be considered as rather good and can be ascribed to the protection of the laccase active structure upon immobilization on the nanohybrid material, providing also a suitable microenvironment for the catalytic activity of the enzyme.

The Lac/rGO/Sb_2O_5/GCE biosensor was finally employed to determine estriol in human urine samples. The concentration of estriol in the human urine samples was measured by triplicate using the standard addition method to minimize the matrix effect. The preparation of the samples consisted only in dilution of an appropriate volume of urine samples with ethanol to a final

Table 1
Comparison of the analytical characteristics reported for electrochemical sensors for the determination of estriol.

Material	Technique	LOD (mol L^{-1})	Linear range (mol L^{-1})	Reference
rGO–SbNPs	DPV	5.0×10^{-10}	2.0×10^{-7} - 1.4×10^{-6}	[34]
MMIPs NPs/CPE	CV	1.0×10^{-7}	6.0×10^{-7} - 1.0×10^{-4}	[35]
BDD	SWV	1.7×10^{-7}	2.0×10^{-7} - 2.0×10^{-5}	[20]
Ni-GCE	CV	1.0×10^{-7}	5.0×10^{-6} - 1.0×10^{-4}	[36]
PPOMC	SWV	5.0×10^{-9}	1.0×10^{-8} - 2.0×10^{-6}	[37]
Pt/MWNTs/GCE	SWV	6.2×10^{-7}	1.0×10^{-6} - 7.5×10^{-5}	[38]
Lac/rGO/Sb_2O_5/GCE	amperommetry	1.1×10^{-8}	2.5×10^{-8} - 1.03×10^{-6}	this work

rGO–SbNPs: reduced graphene oxide-antimony nanoparticles; DPV: differential pulse voltammetry; MMIPs NPs/CPE: magnetic molecularly imprinted nanoparticles in carbon paste electrode; CV: cyclic voltammetry; BDD: Boron-doped diamond electrode; SWV: square-wave voltammetry; Ni-GCE: nickel-modified glassy carbon electrode; PPOMC: poly(L-proline)-ordered mesoporous carbon composite; Pt/MWNTs/GCE: Pt-nanoclusters/multi-walled carbon nanotubes on GCE.

Table 2
Selectivity of the amperometric Lac/rGO/Sb_2O_5/GCE biosensor for estriol.

Species	Concentration	% of signal
Estriol	$1.0 \cdot 10^{-6}$ mol L^{-1}	100
Hydroquinone	10[a]	-[c]
	100[b]	-[c]
Catechol	10	-[c]
	100	1.05
Dopamine	10	-[c]
	100	1.15
Progesterone	10	-[c]
	100	0.92
Bysphenol A	10	-[c]
	100	-[c]
17β-estradiol	10	3.58
	100	101.40
Ethinylestradiol	10	6.16
	100	65.61
Ascorbic acid	10	-[c]
	100	-[c]

[a] 10 times estriol concentration (10 μmol L^{-1}).
[b] 100 times estriol concentration (100 μmol L^{-1}).
[c] undetectable.

Table 3
Determination of estriol in human urine samples by using the Lac/rGO/Sb_2O_5/GCE biosensor.

Sample	Spiked (mmol L^{-1})	Found (mmol L^{-1})	Recovery (%)
Urine A	-	$0.115 \pm 1.1 \times 10^{-3}$	-[a]
Urine A	0.086	$0.201 \pm 2.0 \times 10^{-3}$	100.1 ± 1
Urine B	-	$0.102 \pm 1.0 \times 10^{-3}$	-[a]
Urine B	0.086	$0.188 \pm 1.8 \times 10^{-3}$	100.2 ± 1

[a] undetectable.

volume of 5 mL. The urine sample was obtained from a healthy volunteer, consuming contraceptive pill, in different days of the hormonal cycle (A and B). The obtained results are summarized in Table 3.

A direct relationship was observed for the measured cathodic current and estriol concentration with a high correlation for all the cases (r = 0.999). Recoveries about 100 ± 1% of estriol in human urine samples (n = 3) were obtained after spiking the samples with 86 μmol L^{-1}. These results show fairly well the suitability of the Lac/rGO/Sb_2O_5/GCE biosensor for the analysis of estriol in real samples.

4. Conclusion

A new hybrid nanomaterial with electrocatalytic ability was prepared by coating GO with a Sb_2O_5 thin film through a one-pot reaction scheme. The modification of GO sheets with Sb_2O_5 was confirmed by several techniques. The resulting rGO/Sb_2O_5 nanohybrid showed excellent properties as support for the covalent immobilization of laccase through a glutaraldehyde-mediated cross-linking process. This immobilization strategy was employed to design a nanostructured enzyme biosensor for the amperometric determination of estriol. The synergic effect of GO, Sb(V) oxide and laccase allowed fast and successful electrocatalytic transformation of estriol on the sensing interface, then resulting in a high sensitivity, excellent selectivity and low detection limit for the biosensor device.

This Lac/rGO/Sb_2O_5/GCE biosensor was successfully applied for the rapid determination of estriol in human urine samples with a high performance. These results suggest that this novel graphene-based hybrid nanomaterial could be useful for the design of electrochemical biosensor devices for the determination of estriol in clinical and environmental samples.

Acknowledgments

Financial support from FAPESP (2011/23047-7 and 2014/02457-0), the Spanish Ministry of Science and Innovation (CTQ2011-24355, CTQ2012-34238 and CTQ2014-58989) and the Community of Madrid(S2013/MIT-3029, Programme NANOAVANSENS) is gratefully acknowledged. R. Villalonga acknowledge to Ramón & Cajal contract from the Spanish Ministry of Science and Innovation.

Appendix A. Supplementary data

Supplementary data associated with this article can be found, in the online version, at http://dx.doi.org/10.1016/j.electacta.2015.06.013.

References

[1] K.K. Mistry, K. Layek, A. Mahapatra, C. RoyChaudhuri, H. Saha, A review on amperometric-type immunosensors based on screen-printed electrodes, Analyst 139 (2014) 2289.
[2] P. Yáñez-Sedeño, L. Agüí, R. Villalonga, J.M. Pingarrón, Biosensors in forensic analysis. A review, Anal Chim Acta 823 (2014) 1.
[3] H. Kaur, R. Kumar, J.N. Babu, S. Mittal, Advances in arsenic biosensor development: A comprehensive review, Biosens Bioelectron 63 (2015) 533.
[4] R. Villalonga, C. Camacho, R. Cao, J. Hernández, J.C. Matías, Amperometric biosensor for xanthine with supramolecular architecture, Chem Commun (2007) 942.
[5] J. Kailashiya, N. Singh, S.K. Singh, V. Agrawal, D. Dash, Graphene oxide-based biosensor for detection of platelet-derived microparticles: A potential tool for thrombus risk identification, Biosens Bioelectron 65 (2015) 274.
[6] R. Villalonga, P. Díez, P. Yáñez-Sedeño, J.M. Pingarrón, Wiring horseradish peroxidase on gold nanoparticles-based nanostructured polymeric network for the construction of mediatorless hydrogen peroxide biosensor, Electrochim Acta 56 (2011) 4672.
[7] M. Eguílaz, R. Villalonga, L. Agüí, P. Yáñez-Sedeño, J.M. Pingarrón, Gold nanoparticles: poly (diallyldimethylammonium chloride)–carbon nanotubes composites as platforms for the preparation of electrochemical enzyme biosensors: Application to the determination of cholesterol, J Electroanal Chem (2011) 661.
[8] M. Pumera, Graphene-based nanomaterials and their electrochemistry, Chem Soc Rev 39 (2010) 4146.
[9] E. Araque, R. Villalonga, M. Gamella, P. Martinez-Ruiz, J. Reviejo, J.M. Pingarron, Crumpled reduced graphene oxide-polyamidoamine dendrimer hybrid nanoparticles for the preparation of an electrochemical biosensor, J Mater Chem B 1 (2013) 2289.
[10] E. Araque, R. Villalonga, M. Gamella, P. Martinez-Ruiz, A. Sanchez, V. Garcia-Baonza, J.M. Pingarron, Water-soluble reduced graphene oxide-carboxymethylcellulose hybrid nanomaterial for electrochemical biosensor design, ChemPlusChem 79 (2014) 1334.
[11] A. Boujakhrout, A. Sánchez, P. Díez, S. Jimenez, P. Martínez-Ruiz, M. Peña-Álvarez, J.M. Pingarrón, R. Villalonga, Decorating graphene/nanogold with dextran-based polymer brushes for the construction of ultrasensitive electrochemical enzyme biosensors, J Mat Chem B 3 (2015) 3518.
[12] E. Araque, C.B. Arenas, M. Gamella, J. Reviejo, R. Villalonga, J.M. Pingarrón, Graphene-polyamidoamine dendrimer-Pt nanoparticles hybrid nanomaterial for the preparation of mediatorless enzyme biosensor, J Electroanal Chem 717–718 (2014) 96.
[13] L. Meng, Y. Xia, W. Liu, L. Zhang, P. Zou, Y. Zhang, Hydrogen microexplosion synthesis of platinum nanoparticles/nitrogen doped graphene nanoscrolls as new amperometric glucose biosensor, Electrochim Acta 152 (2015) 330.
[14] Z.S. Wu, G.M. Zhou, L.C. Yin, W. Ren, F. Li, H.M. Cheng, Graphene/metal oxide composite electrode materials for energy storage, Nano Energy 1 (2012) 107.
[15] T.C. Canevari, R.C.G. Vinhas, R. Landers, Y. Gushikem, SiO2/SnO2/Sb2O5 microporous ceramic material for immobilization of Meldola's blue: Application as an electrochemical sensor for NADH, Biosens Bioelectron 26 (2011) 2402.
[16] C.M. Maroneze, R.C.S. Luz, R. Landers, Y. Gushikem, SiO2/TiO2/Sb2O5/graphite carbon ceramic conducting material: preparation, characterization, and its use as an electrochemical sensor, J Solid State Electr 14 (2010) 115.
[17] G. Zaitseva, Y. Gushikem, E.S. Ribeiro, S.S. Rosatto, Electrochemical property of methylene blue redox dye immobilized on porous silica-zirconia-antimonia mixed oxide, Electrochim Acta 47 (2002) 1469.
[18] L.Q. Luo, F. Li, L.M. Zhu, Y.P. Ding, D.M. Deng, Electrochemical sensing platform of natural estrogens based on the poly(L-proline)-ordered mesoporous carbon composite modified glassy carbon electrode, Sensor Actuat B-Chem 187 (2013) 78.
[19] J. Piwowarska, S. Radowicki, J. Pachecka, Simultaneous determination of eight estrogens and their metabolites in serum using liquid chromatography with electrochemical detection, Talanta 81 (2010) 275.

[20] K.D. Santos, O.C. Braga, I.C. Vieira, A. Spinelli, Electroanalytical determination of estriol hormone using a boron-doped diamond electrode, Talanta 80 (2010) 1999.
[21] M. Gorga, S. Insa, M. Petrovic, D. Barcelo, Analysis of endocrine disrupters and related compounds in sediments and sewage sludge using on-line turbulent flow chromatography-liquid chromatography-tandem mass spectrometry, J Chromatogr A 1352 (2014) 29.
[22] N. Andrasi, A. Helenkar, A. Vasanits-Zsigrai, G. Zaray, I. Molnar-Perl, The role of the acquisition methods in the analysis of natural and synthetic steroids and cholic acids by gas chromatography-mass spectrometry, J Chromatogr A 1218 (2011) 8264.
[23] J. Lu, J. Wu, P.J. Stoffella, P.C. Wilson, Isotope dilution-gas chromatography/mass spectrometry method for the analysis of alkylphenols, bisphenol A, and estrogens in food crops, J Chromatogr A 1258 (2012) 128.
[24] Y.P. Tang, S.Q. Zhao, Y.S. Wu, J.W. Zhou, M. Li, A direct competitive inhibition time-resolved fluoroimmunoassay for the detection of unconjugated estriol in serum of pregnant women, Anal Methods 5 (2013) 4068.
[25] J.H. Zhou, Z.J. Sui, J. Zhu, P. Li, C. De, Y.C. Dai, W.K. Yuan, Characterization of surface oxygen complexes on carbon nanofibers by TPD, XPS and FT-IR, Carbon 45 (2007) 785.
[26] G.H. Zhou, Y.Z. Liu, M. Luo, Q.F. Xu, X.H. Ji, Z.K. He, Peptide-capped gold nanoparticle for colorimetric immunoassay of conjugated abscisic acid, ACS Appl Mater Interfaces 4 (2012) 5010.
[27] S.H. Wang, S.L. Lin, L.Y. Du, H.S. Zhuang, Electrochemical enzyme-linked immunoassay for the determination of estriol using methyl red as substrate, Anal Lett 39 (2006) 947.
[28] W.S. Hummers, R.E. Offeman, Preparation of graphitic oxide, J Am Chem Soc 80 (1958) 1339.
[29] M. Ciszewski, A. Mianowski, G. Nawrat, P. Szatkowski, Reduced graphene oxide supported antimony species for high-performance supercapacitor electrodes, ISRN Electrochemistry 2014 (2014) 826832.
[30] R.A. Nistor, D.M. Newns, G.J. Martyna, The role of chemistry in graphene doping for carbon-based electronics, ACS Nano 5 (2011) 3096.
[31] T.C. Canevari, P.A. Raymundo-Pereira, R. Landers, E.V. Benvenutti, S.A.S. Machado, Sol-gel thin-film based mesoporous silica and carbon nanotubes for the determination of dopamine, uric acid and paracetamol in urine, Talanta 116 (2013) 726.
[32] R.S. Ruoff, W.Q. Ding, R. Piner, S. Stankovich, Remarkable mechanics of extremely thin graphite platelets, Abstr Pap Am Chem S 229 (2005) U1146.
[33] E. Dempsey, D. Diamond, A. Collier, Development of a biosensor for endocrine disrupting compounds based on tyrosinase entrapped within a poly(thionine) film, Biosens Bioelectron 20 (2004) 367.
[34] I. Cesarino, F.H. Cincotto, S.A.S. Machado, A synergistic combination of reduced graphene oxide and antimonynanoparticles for estriol hormone detection, Sensors and Actuators B 210 (2015) 453.
[35] L.L. Zhu, Y.H. Cao, G.Q. Cao, Electrochemical sensor based on magnetic molecularly imprinted nanoparticles at surfactant modified magnetic electrode for determination of bisphenol A, Biosens Bioelectron 54 (2014) 258.
[36] G.W. Muna, A. Kaylor, B. Jaskowski, L.R. Sirhan, C.T. Kelley, Electrocatalytic oxidation of estrogenic phenolic compounds at a nickel-modified glassy carbon electrode, Electroanalysis 23 (2011) 2915.
[37] J.C. Song, J. Yang, X.M. Hu, Electrochemical determination of estradiol using a poly(L-serine) film-modified electrode, J Appl Electrochem 38 (2008) 833.
[38] X.Q. Lin, Y.X. Li, A sensitive determination of estrogens with a Pt nano-clusters/multi-walled carbon nanotubes modified glassy carbon electrode, Biosens Bioelectron 22 (2006) 253.